2022 44th Annual International Conference of
the IEEE Engineering in Medicine & Biology Society (EMBC)
Scottish Event Campus, Glasgow, UK, July 11-15, 2022

2022 44th Annual International Conference of the IEEE Engineering in Medicine & Biology Society (EMBC) | 978-1-7281-2782-8/22/$31.00 ©2022 IEEE | DOI: 10.1109/EMBC48229.2022.9871350

Monte Carlo Simulation of the Effect of Human Skin Melanin in Light-Tissue Interactions*

Raghda Al-Halawani[1], Subhasri Chatterjee[1], Panayiotis. A. Kyriacou[1], *Senior Member, IEEE*

Abstract— **Recent reports have highlighted the potential challenges skin pigmentation can have in the accurate estimation of arterial oxygen saturation when using a pulse oximeter. Pulse oximeters work on the principle of photoplethysmography (PPG), an optical technique used for the assessment of volumetric changes in vascular tissue. The primary aim of this research is to investigate the effect of melanin on tissue when utilising the technique of PPG. To address this, a Monte Carlo (MC) light-tissue interaction model is presented to explore the behaviour of melanin in the visible range in the epidermis. A key novelty in this paper is the ability to model the Modified Beer Lambert Law (MBLL) through a fully functional three-dimensional (3D) model in reflective optical geometry. Maximum photon penetration depth was achieved by red light, however limited bio-optical information was retrieved by moderately and darkly pigmented skin at source-detector separations of less than 3 mm. The current MC model can be modified to provide a more realistic representation of absorption and scattering processes in skin.**

I. Introduction

The field of tissue optics is continuously developing as it proves pertinent in medical diagnostics. As a result, there lies a huge focus on designing more advanced technologies to retrieve important information about light-tissue interactions through non-invasive techniques, such as photoplethysmography (PPG). When an optical source is placed on the surface of a volume of tissue, multiple interactions occur before light is transmitted and detected by a photodetector. The resulting waveforms represent the changes in light absorption from non-pulsatile components (DC PPG) such as melanin, muscle, venous blood, etc., and pulsatile blood between the systolic and diastolic phases of the heart (AC PPG).

Monte Carlo models (MCM) have been extensively used as a computational tool to study vital aspects of light-tissue interactions in PPG. It is a mathematical technique which involves modelling the probability of different outcomes with random variables. In comparison to other methods such as random walk theory, diffusion approximation etc., it accounts for the stochastic nature of turbid media, such as single or multi-layered biological tissue.

A. Absorption and Beer Lambert Law

Photon absorption can occur in two different forms; radiative and non-radiative. The latter involves the emission of heat after relaxation of the photon to the ground state, and is employed in the following MCM. All skin chromophores, such as melanin, water, etc., are capable of absorbing a certain number of photons per unit distance. This is characterised by the absorption coefficient ($\boldsymbol{\mu_a}$), which is wavelength dependent. The intensity of light, which is assumed constant after transmitted across the tissue boundary, is given by [2]:

$$\mathbf{I_t = I_0 e^{-\mu_a * L} = I_0 e^{-\varepsilon * C * L}}. \quad (1)$$

Where $\boldsymbol{\varepsilon}$ is the molar extinction coefficient of a medium, C is the concentration of the medium, and L is the total path length of photons travelling through the medium.

The absorbance (A), which is the amount of light absorbed by a medium, is given by the ratio of the intensity of transmitted and incident light [2]:

$$A = \mu_a * L = \varepsilon * C * L. \quad (2)$$

B. Scattering and the Modified Beer Lambert Law

The number of scattering events per unit distance is characterised by the scattering coefficient (μ_s), which is also wavelength dependent. Similarly, scattering can take two different forms, namely elastic and inelastic scattering. The former causes a change in the direction of light propagation due to collisions between scattered particles while preserving kinetic energy [2], which is more relevant to the intended application. The type of scattering that occurs depends on the microphysical properties of the particles or molecules. The model is simulated such that it undergoes Mie scattering and

*This work was not supported by any organisation.

[1] Raghda Al-Halawani is with the Research Centre for Biomedical Engineering, City, University of London, UK, EC1V 0HB. Raghda.al-halawani@city.ac.uk

[1] Subhasri Chatterjee was with the Research Centre for Biomedical Engineering, City, University of London, UK, EC1V 0HB. subhasri.chatterjee.1@city.ac.uk

[1] Panayiotis. A. Kyriacou is with the Research Centre for Biomedical Engineering, City, University of London, UK, EC1V 0HB. p.kyriacou@city.ac.uk

hence, the Henyey-Greenstein phase function is used to present the relationship between the angle of deflection (θ) and the anisotropic factor (*g*), to determine photon directionality [3]:

$$p(\theta) = \frac{1-g^2}{4\pi(1-2g\cos\theta+g^2)^{\frac{3}{2}}}. \quad (3)$$

The amount of light lost due to scattering is denoted by a parameter, G [2]:

$$A = \mu_a * L + G = \varepsilon * C * L + G. \quad (4)$$

The aim of this paper is to explore light-tissue interactions underlying the PPG technique on a basic level, as they have shown to be inadequate in analysing the complex light-tissue interactions in biological tissue [1]. To one's knowledge, the effect of melanin concentration on these interactions have not yet been fully explored, despite reports suggesting the existence of bias in oximetry measurement on subjects with different skin pigmentation since the 1980's [4-8].

II. Materials and Methods

A. Region on interest

The epidermal layer of a finger, with a thickness (t) of 0.25 mm [1] is modelled for three different wavelengths. These include blue light (450 nm), green light (550 nm), and red light (650 nm). The epidermis contains only a specific concentration of melanin and water; however, the presence of water is disregarded for model simplification. The author in [9] provides the volume fractions of melanosomes (V_{mel}) in the human epidermis:

Description	V_{mel} (%)
Light-skinned adults	1.3 – 6.3
Moderately pigmented adults	11 – 16
Darkly pigmented adults	18 – 43

Table 1: Volume fraction of melanosomes in the epidermis for different skin pigments.

The MCM was simulated for a V_{mel} range of 5% - 20%, increasing in increments of 5%, in an attempt to investigate light-tissue interactions across the entire range of human skin pigments. The total sample size of the study was 12 (4 melanin concentrations simulated at 3 different wavelengths).

Firstly, the absorption coefficients of melanin at different wavelengths were calculated [9]:

$$\mu_{a_{mel}}\,(mm^{-1}) = 6.6 * 10^{10} * \lambda^{-3.33}. \quad (5)$$

Secondly, the skin baseline was assumed to be the same as bloodless rat skin, as the epidermis is an avascular skin layer. Therefore, the absorption coefficient was calculated [9]:

$$\mu_{a_{skinbaseline}} = 7.84 * 10^{7} * \lambda^{-3.255}. \quad (6)$$

Combining (5) and (6), the absorption coefficient of the epidermis was computed [9]:

$$\mu_{a_{epidermis}} = V_{mel} * \mu_{a_{mel}} + (1 - V_{mel}) * \mu_{a_{skinbaseline}}. \quad (7)$$

The scattering coefficient of the epidermis alone (and not the combined sublayers of skin) was difficult to retrieve from secondary sources. In addition, the inability to obtain data experimentally imposed greater challenges regarding the simulation of a relatively accurate model. As a result, some assumptions were made to approximate $\mu_{s_{epidermis}}$. Some experimental data [10] has shown that over the visible spectrum, the reduced-scattering coefficient ($\mu_{rs_{epidermis}}$) of the epidermis was always $2 - 3\ mm^{-1}$ higher than the reduced-scattering coefficient of the dermis. To calculate μ_{rs}, the following equation is used:

$$\mu_{rs} = \mu_s * (1 - g). \quad (8)$$

Therefore, by assuming that $\mu_{s_{epidermis}}$ is $3\ mm^{-1}$ smaller than $\mu_{s_{dermis}}$ (since absorption by melanin dominates in the epidermis), data for the scattering coefficients of the epidermis was estimated from [11]. Moreover, the simulation was limited to the reliable retrieval of data of the anisotropic factors of the epidermis at the selected wavelengths. Instead, the anisotropic factors of skin at similar wavelengths [12, 13] were used to estimate *g*.

B. Monte Carlo simulation procedure

Tissue	λ (nm)	μ_s (mm^{-1})	g
Human epidermis	450	9.41	0.8
	550	4.722	0.85
	650	2.598	0.9

Table 2: Scattering coefficients and anisotropic factors of the epidermis for blue, green, and red light.

The Monte Carlo procedure explained in [2, 14] provided the theory, processes, and equations to simulate a multi-layered MCM as photons travelled from the source and across all the interactions sites until detected. This model was adapted to create the current monolayer MCM. A set of conditions were implemented to govern the movement of 10^8 photons (N) through the tissue. The code was written using the functions 'rand', 'while', 'for', 'if', 'elseif', and 'else' in MATLAB. The model parameters were: μ_a (of the epidermis and melanin), μ_s and g (of the epidermis only), N, n (of the epidermis and air), and V_{mel}.

To account for scattering, the spherical nature of the photons was represented using the Cartesian coordinates x, y, z (Fig. 1). In reflective optical geometry, the source-detector separation (*d*) was adjusted by increasing the distance between the lateral (x) direction relative to a collimated beam from a point source (S) i.e., located at (0,0,0) and the photodetector (D). Photons were launched perpendicular to the surface of the epidermis.

Figure 2 shows a vector ($\vec{r}$) which denotes the instantaneous direction of a photon, makes angles α, β, and γ with the x, y, and z axes, respectively. Therefore, all the position vectors, which are defined by their direction cosines (u_x, u_y, u_z), were converted with respect to the Cartesian coordinate system to the spherical polar coordinate system:

$$u_x = \sin\theta\cos\varphi. \,,\, u_y = \sin\theta\sin\varphi. \,,\, u_z = \cos\theta. \quad (9)$$

$$\theta = 2 * \xi * \sin^{-1}(\mathrm{NA}). \,,\, \varphi = 2 * \xi * \pi. \quad (10)$$

where NA = numerical aperture, a dimensionless number that provides the range of angles over which the source or detector can accept or emit light.

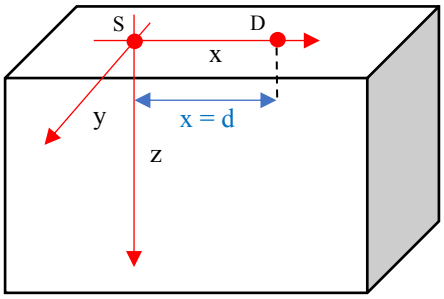

Fig. 1 Illustration of the Cartesian coordinate system and reflectance PPG adapted from [2]

Furthermore, a photon was launched with an initial weight equal to unity. The amount of light lost at the tissue surface (R_f) due to the differences in refractive indices (n_{air}, n_{tissue}) was subtracted from the photon's initial weight before it entered the epidermis:

$$\left(\frac{n_{air}-n_{tissue}}{n_{air}+n_{tissue}}\right)^2 \quad (11)$$

The photon moved a random distance (l) using a random number (ξ), which combined the effects of absorption and scattering (the attenuation coefficient, μ_t), to achieve the most realistic photon distribution within the tissue [14]:

$$l = \frac{-\ln(\xi)}{\mu_a+\mu_s} = \frac{-\ln(\xi)}{\mu_t}. \quad (12)$$

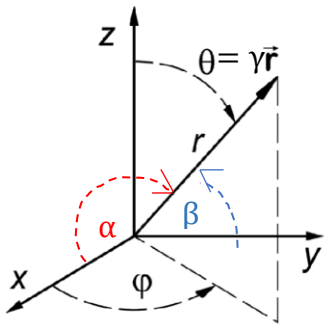

Fig. 2 The relationship between the spherical polar coordinate and Cartesian coordinate system adapted from [2].

This was used to calculate the new position coordinates (x_2, y_2, z_2) of the photon along with the direction cosines, respectively [2]:

$$x_2 = x + l * u_x. \,,\, y_2 = y + l * u_y. \,,\, z_2 = z + l * u_z. \quad (13)$$

Once a photon was backscattered to the photodetector located on the tissue surface (z=0), a conditional 'if' loop was used to check whether the photon was detected by the photodetector i.e., if the photon satisfied the survival criteria. The x and y coordinates of a transmitted photon were computed (14), and used to determine whether the photon was detected by calculating the size of the photon (15), and the angle of acceptance (16) [2]:

$$x_3 = z * \frac{u_x}{u_z} + x. \,,\, y_3 = z * \frac{u_y}{u_z} + y. \quad (14)$$

$$x_3{}^2 + y_3{}^2 < r^2. \quad (15)$$

$$\theta_{acc} = \sin^{-1}(\mathrm{NA}). \quad (16)$$

To reduce statistical uncertainty, implicit photon capture, a variance reduction technique, was used to improve the efficiency of the MC simulation by considering a 'photon cluster' instead of a single photon entering the tissue [14]. If a photon cluster did not hit the boundary, a fraction of its weight was absorbed (wa), and the remainder continued to travel to the next interaction site [14]:

$$wa = \left(\frac{\mu_a}{\mu_t}\right) * w = \Lambda * w. \quad (17)$$

A vector 'killw' was also created to record all the terminated photons if a) they were transmitted but not detected or b) the weight of the photon cluster did not exceed the pre-defined weight threshold (10^{-4}) i.e., intensity was negligible due to continuous absorption. If the remainder of a photon cluster, given by w = w – wa [2], was not transmitted, detected, or terminated, then it was scattered. The direction cosines of these photons were only updated if they were not extremely close to the z axis, using the following relationships [15]:

$$u_{x1} = \frac{\sin\theta(u_x u_z\cos\varphi - u_y\sin\varphi)}{\sqrt{1-u_z{}^2}} + u_x\cos\theta. \,,$$
$$u_{y1} = \frac{\sin\theta(u_y u_z\cos\varphi + u_x\sin\varphi)}{\sqrt{1-u_z{}^2}} + u_y\cos\theta \,,$$
$$u_{z1} = -\sin\theta\cos\varphi\sqrt{1-u_z{}^2} + u_z\cos\theta. \quad (18)$$

III. Results and Discussion

For all wavelengths, maximum penetration depth was achieved when V_{mel} = 5%. For a multi-layered finger model [1], one could see beyond the dermal sublayers when λ = 450 nm (0.98 mm), and possibly the first layer of fat when λ = 550 nm (2.06 mm), and even more so when λ = 650 nm (3.42 mm). Hence, retrieval of bio-optical information for moderately and darkly pigmented subjects was limited. As expected, blue light was mostly absorbed by melanin at all concentrations and hence, *d* did not exceed 1 mm.

It can be seen that light absorption increases as melanin concentration increases, resulting in a progressive reduction in photon detection (Fig. 3(a)). Adjusting the source-detector separation to 3 mm (Fig. 3(b)) leads to negligible outcomes when V_{mel} = 10% - 20%, proving impractical for reflectance PPG applications such as pulse oximetry in consumer products. This may justify why calibration curves for such devices are generated on majority lightly pigmented subjects.

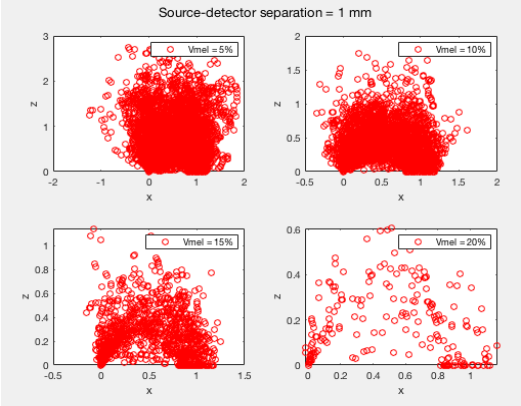

(a)

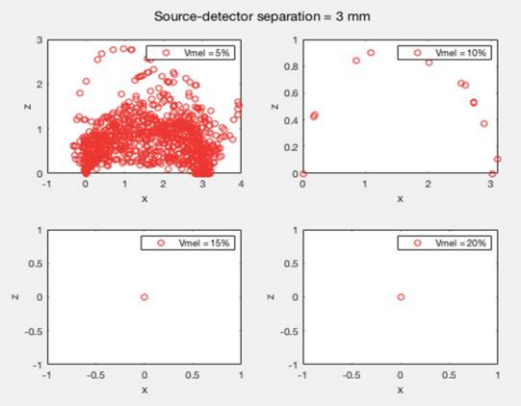

(b)

Fig. 3 (a) Photon propagation of red light when d = 1 mm for different skin pigmentations. (b) Photon propagation of red light when d = 3 mm for different skin pigmentations. The x axis shows the movement of photons from source to detector, and the z axis shows the penetration depth of photons.

Moreover, the modified Beer Lambert Law (MBLL) is successfully demonstrated in Figure 4, as the linear relationship between absorbance and melanin concentration remains true for a scattering medium at different source-detector separations. The y-intercepts (G values) depend on the system parameters i.e. the optical properties of the epidermis and the sensor geometry. Hence, negative G values

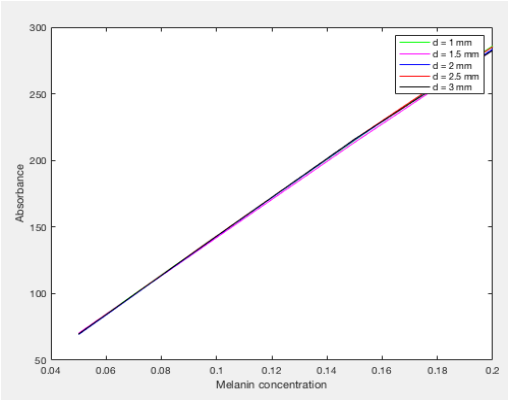

Fig. 4 Verification of MBLL: Linear relationship between absorbance and melanin concentration.

may indicate the dominance of absorption in the epidermal layer of the human finger. Further work is needed to understand the relationship between G, underlying absorption by melanin and other skin chromophores, and scattering processes in the skin. This may help justify outcomes in Monte Carlo models for specific applications, including the extended modified Beer Lambert law [16].

IV. Conclusion

This paper has presented a Monte Carlo model of the human epidermis to analyse the behaviour of light, namely the differences in optical path length, photon penetration depth, etc., in reflective optical geometry. The results have successfully complied with the principles of tissue optics, specifically the modified Beer Lambert law. Visible light is highly absorbed by melanin, especially as the source-detector separation increases. It is clear that retrieval of bio-optical information from moderately and darkly pigmented subjects is limited.

The current MCM can be modified to provide a more realistic representation of skin by assessing the impact of absorption and scattering in the dermis due to the presence of blood, water, and lipids. Other modifications include removal of the point source to provide defined source dimensions for experimental purposes. Overall, such MCM may be utilised to predict the behaviour of photons under the influence of melanin in tissue.

References

[1] S. Chatterjee, P. A. Kyriacou. (2019, February). "Monte Carlo Analysis of Optical Interactions in Reflectance and Transmittance Finger Photoplethysmography", *Sensors (Basel)*. vol. 19, issue 4.

[2] S. Chatterjee, "Monte Carlo Investigation of Light-Tissue Interaction in Photoplethysmography," Ph.D. dissertation, Dept. Elect. Eng., City Univ., London, 2018.

[3] V. Tuchin (2007). Tissue Optics: Light Scattering Methods and Instruments for Medical Diagnosis, vol. 13, SPIE press Bellingham.

[4] A. L. Ries, L. M. Prewitt, J. J. Johnson. (1989, August). "Skin color and ear oximetry", *Chest.* vol. 96, issue 2, pp. 287-90.

[5] P. E. Bickler, J. R. Feiner, J. W. Severinghaus. (2005, April). "Effects of skin pigmentation on pulse oximeter accuracy at low saturation", *Anesthesiology*. vol 102, pp. 715–719.

[6] M. W. Sjoding, R. P. Dickson, T. J. Iwashyna, S. E. Gay, T. S. Valley (2020, December). "Racial Bias in Pulse Oximetry Measurement", *N Engl J Med* ; 383: 2477–2478.

[7] Z. Vesoulis, A. Tims, H. Lodhi, N. Lalos, H. Whitehead. "Racial discrepancy in pulse oximeter accuracy in preterm infants", *J Perinatol* [In Press], 2021.

[8] M. D. Wiles, A. El-Nayal, G. Elton, et al. "The effect of patient ethnicity on the accuracy of peripheral pulse oximetry in patients with COVID-19 pneumonitis: a single-centre, retrospective analysis", *Anaesthesia* [In Press], 2021.

[9] S. L. Jacques. (1998, January). "Skin Optics summary." *Oregon Medical Laser Center News* [Online]. Available: https://omlc.org/news/jan98/skinoptics.html

[10] T. Lister, P. A. Wright, P. H. Chappell. (2012, September). "Optical properties of human skin." *Journal of Biomedical Optics* [Online]. vol. 17, issue 9.

[12] A. N. Bashkatov, E. A. Genina, and V. V. Tuchin. (2011, January). "Optical properties of skin, subcutaneous, and muscle tissues: A review." *Journal of Innovative Optical Health Sciences* [Online]. vol. 4, issue 1, pp. 9-38.

[12] S. Chatterjee, K. Budidha, P. A. Kyriacou. (2020, September). "Investigating the origin of photoplethysmography using a multiwavelength Monte Carlo model." *Physiological Measurement* [Online]. vol 41, issue 8.

[13] J. P. Phillips, P. A. Kyriacou, and D. P. Jones, "Calculation of Photon Path Changes due to Scatter in Monte Carlo Simulations", in *Annual International Conference of the IEEE Engineering in Medicine and Biology Society*, London, 2010.

[14] L. Wang, S. L. Jacques, and L. Zheng. (1995, July). "MCML – Monte Carlo modelling of light transport in multi-layered tissues." *Computer Methods and Programs in Biomedicine* [Online]. vol. 47, issue 2, pp. 131 - 146.

[15] E. D. Cashwell, C. J. Everett, *A practical manual on the Monte Carlo method for random walk problems*, Los Alamos, New Mexico: Los Alamos Scientific Laboratory of the University of California, 1957.

[16] A. Huong and X. Ngu. (2014, May). ''The application of extended modified lambert beer model for measurement of blood carboxyhemoglobin and oxyhemoglobin saturation,'' *J. Innov. Opt. Health Sci* [Online]. vol. 7, issue 3.